



Contents lists available at ScienceDirect

Bioorganic & Medicinal Chemistry Letters

journal homepage: www.elsevier.com/locate/bmcl



3-(Pyridin-2-yl-ethynyl)benzamide metabotropic glutamate receptor 5 negative allosteric modulators: Hit to lead studies

Adam M. Gilbert^{*}, Matthew G. Bursavich, Sabrina Lombardi, Adedayo Adedoyin, Jason M. Dwyer, Zoe Hughes, Jeffrey C. Kern, Xavier Khawaja, Sharon Rosenzweig-Lipson, William J. Moore, Sarah J. Neal, Michael Olsen, Stacey J. Sukoff Rizzo, Dane Springer

Pfizer Global Research and Development, Groton Laboratories, Eastern Point Road, Groton, CT 06340, USA

ARTICLE INFO

Article history:

Received 4 October 2010
Revised 3 November 2010
Accepted 4 November 2010
Available online 12 November 2010

Keywords:

mGluR5
Negative allosteric modulator
Anxiolytic
LipE

ABSTRACT

A series of 3-(pyridin-2-yl-ethynyl)benzamide negative allosteric modulators of the metabotropic glutamate receptor 5 (mGluR5 NAMs) have been prepared. Starting from HTS hit **1** (IC₅₀: 926 nM), potent mGluR5 NAMs showing excellent potencies (IC₅₀s <50 nM) and good physicochemical profiles were prepared by monitoring LipE values. One compound **26** showed excellent mGluR5 binding (K_i: 21 nM) and antagonism (IC₅₀: 8 nM), an excellent rat PK profile (CL: 12 mL/min/kg, %F: 85) and showed oral activity in a mouse 4-Plate Behavioral model of anxiety (MED: 30 mpk) and a mouse Stress Induced Hyperthermia model of anxiety (MED 17.8 mpk).

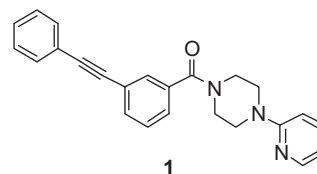
© 2010 Elsevier Ltd. All rights reserved.

Glutamate is a prominent neurotransmitter which exerts its effects via ionotropic and metabotropic glutamate receptors. The metabotropic glutamate receptors (mGluRs) are characterized as having a seven transmembrane (7TM) α -helical domain, that is, connected via a cysteine-rich large extracellular amino-terminal domain. The orthosteric binding site of the mGluRs is contained in the amino-terminal domain, whereas the allosteric binding sites that have been identified to date reside in the hydrophobic 7TM domain.¹

Metabotropic glutamate receptors (mGluRs) are members of the G protein-coupled receptor (GPCR) family C, which is distinguished from other GPCR families by its large extracellular N-terminal agonist binding site. There are eight subtypes of mGluRs (Group I: mGluR1 and mGluR5; Group II: mGluR2 and mGluR3; Group III: mGluRs 4, 6, 7, 8) based on their sequence homology, pharmacology and coupling to effector mechanisms.² The Group I receptor mGluR5 is post-synaptically expressed at high levels in brain regions thought to be involved in anxiety,³ and antagonism of these receptors signaling is expected to reduce hyperactive glutamatergic signaling in these regions.⁴ Thus there has been a significant effort over the past 10 years to identify selective and efficacious mGluR5 antagonists with most of the effort focusing on finding negative allosteric modulators (mGluR5 NAMs) that bind to the hydrophobic 7TM domain as attempts to find

selective brain penetrant orthosteric antagonists have been unsuccessful.⁵

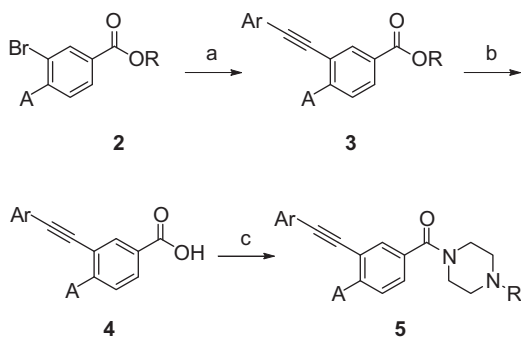
To look for novel mGluR5 NAMs, a high-throughput screen was conducted using a FLIPR Ca²⁺ mobilization assay in a rat mGluR5/HEK-293 cell line containing an EC₉₀ concentration of L-glutamate. Aryl acetylene **1** was identified as a moderately potent mGluR5 NAM (K_i: 139 nM, IC₅₀: 926 nM) with a low LipE (2.4) and several physicochemical property issues (Table 1). Herein we describe the hit to lead optimization of **1** to potent mGluR5 NAMs with improved physicochemical properties, good oral bioavailability and significant in vivo activity.



The major synthetic route to 3-(aryl ethynyl)benzamide mGluR5 NAMs is described in Scheme 1.⁶ Thus commercially available methyl 3-bromobenzoates **2** are coupled with aryl alkynes using standard Sonagashira–Castro–Stephens coupling conditions to produce **3**.⁷ Hydrolysis of the ester with NaOH gives the corresponding acids **4** which are then converted to the piperazine amides

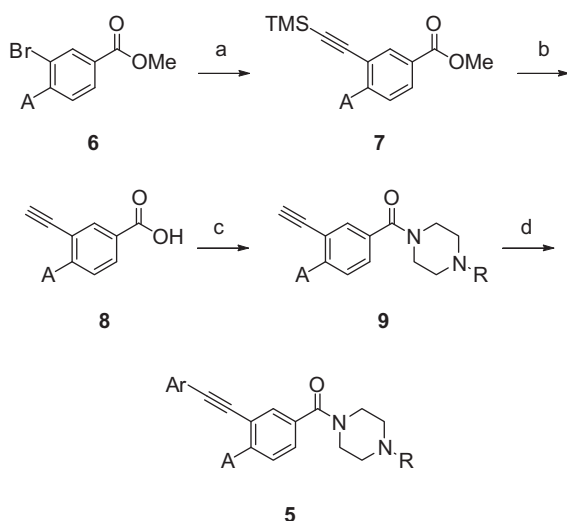
^{*} Corresponding author. Tel.: +1 860 715 6275; fax: +1 860 686 5507.

E-mail address: adam.gilbert@pfizer.com (A.M. Gilbert).



Scheme 1. Reagents and conditions: (a) ArCCH , cat. $\text{PdCl}_2(\text{PPh}_3)_2$, CuI , TEA, DMF, 23 °C; (b) NaOH, EtOH, 23 °C; (c) *R*-piperazine, EDCI, HOBt, TEA, CH_2Cl_2 , 23 °C.

using EDCI/HOBt coupling conditions.⁸ In cases where the aryl acetylene is not commercially available, the route shown in Scheme 2 was used. Thus methyl bromobenzoates **6** are coupled with ethynyltrimethylsilane using Sonagashira–Castro–Stephens conditions to



Scheme 2. Reagents and conditions: (a) ethynyltrimethylsilane, $\text{PdCl}_2(\text{Ph}_3\text{P})_2$, CuI , TEA, 80 °C; (b) KOH, EtOH, H_2O , 50 °C; (c) *R*-piperazine, EDCI, DMAP, *i*-Pr₂EtN, CH_2Cl_2 , 23 °C; (d) ArBr , $\text{PdCl}_2(\text{CH}_3\text{CN})_2$, XPhos, Cs_2CO_3 , MeCN, 80 °C.

give **7**.⁹ Acid hydrolysis with concomitant desilylation produces alkyne acids **8**.¹⁰ EDCI/HOBt coupling⁸ produces **9**, and the terminal acetylene substituent is incorporated with via another Sonagashira–Castro–Stephens coupling to produce **5**.⁷

Binding of compounds to the mGluR5 receptor was assessed by measuring displacement of [³H]-2-methyl-6-(phenylethyl)pyridine (MPEP), a known mGluR5 antagonist that binds to the trans-membrane allosteric binding site, from HEK-293 cell membranes that express the rat mGluR5 receptor. Functional antagonism of mGluR5 was determined by a FLIPR assay using rat mGluR5/HEK-293 cells in the presence of an EC₉₀ concentration of L-glutamate. In vivo efficacy was assessed using two mouse behavioral models predictive of anxiolytic-like activity, the Four-Plate assay (4-Plate) and Stress Induced Hyperthermia model (SIH). Aqueous solubility, cytochrome P450 (CYP) and rat liver microsome (RLM) stability measurements were determined according to methods summarized by Kerns and Di.¹¹

The HTS hit **1** displays modest mGluR5 binding affinity and functional antagonism (Table 1). Moreover, **1** possesses poor aqueous solubility, moderate CYP inhibition and poor rat liver microsome (RLM) stability. The low LipE¹² for **1** is consistent with this poor physicochemical profile (LipE: 2.4). Replacement of the acetylene moiety with $-\text{CH}=\text{CH}-$, $-\text{OCH}_2-$ or removing it altogether produces weakly active compounds (data not shown). Substitution of the $\text{R}^1 = \text{Ph}$ with 3-OMe (**10**), 3-H₂N (**11**), 4-OMe (**12**), 4-Me (**13**) or Bn (**14**) produces compounds showing comparatively weaker affinity and functional antagonism compared to **1**. The physicochemical properties of these analogs show little improvement as well. Replacement of the $\text{R}^1 = \text{Ph}$ with a 2-Pyr group produces **15** which shows improved affinity, antagonism, aqueous solubility and CYP profile. Optimization of the physicochemical profile in **15** is consistent with an increase of LipE values from **1** (2.4) to **15** (4.1).

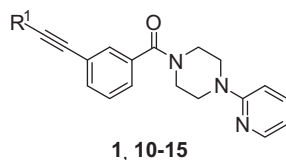
Variation of the R^3 (piperazine) substituent also has an effect on mGluR5 affinity and antagonism (Table 2). Adding nitrogen to the 2-pyridinyl ring of **1** (**16** 2-pyrazine, **17** 2-pyrimidine) to increase aqueous solubility produces a reduction in mGluR5 affinity and potency. The addition of a 5-Me group to the 2-pyridinyl in **1** produces **18** (R^3 : 5-Me, 2-pyridinyl) which shows an improvement in binding and antagonism (K_i : 65 nM, IC₅₀: 181 nM), an improvement in RLM stability ($t_{1/2}$: 13 min), but aqueous solubility is poor (1 μg/mL) and CYP3A4 and CYP2C9 show ≥45% inhibition @ 3 μM. A marked improvement in affinity/functional inhibition and RLM stability is seen for compounds when $\text{R}^2 = \text{OMe}$. Compounds

Table 1
 R^1 terminal alkyne mGluR5 negative allosteric modulator derivatives **1**, **10–15**

Compds	R^1	mGluR5		Aq solubility (μg/mL)	CYP inhibition, 3A4, 2D6, 2C9 (% inhib. @ 3 μM)	RLM stability, $t_{1/2}$ (min)	LipE ^b
		K_i^a (nM)	IC ₅₀ ^a (nM)				
1	Ph	139	926	0.5	48, 5, 50	3	2.4
10	(3-OMe)Ph	212	10,000	1	81, 11, 60	3	2.3
11	(3-NH ₂)Ph	430	10,000	1	94, 5, 58	2	3.1
12	(4-OMe)Ph	2360	nd	1	80, 8, 79	4	1.3
13	(4-Me)Ph	1906	nd	3	70, 3, 65	5	0.8
14	Benzyl	139	163	6	4, 85, 2	4	2.3
15	2-Pyridine	96	172	51	31, 1, 22	5	4.1

^a Values are means of two experiments, standard deviations are ±10%.

^b LipE is calculated using mGluR5 IC₅₀ values.



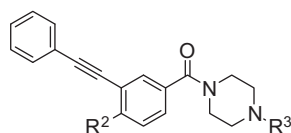
19–22 (R^3 : **19** 2-pyridine, **20** 2-pyrazine, **21** 2-pyrimidine, **22** 5-Me-2-pyridine) all show improved binding affinity compared to the $R^2 = H$ analogs (**1**, **16–20**) and improved RLM stability. Two compounds where $R^2 = Me$ (R^3 : **23** 2-pyridine, **24** 2-pyrazine) also showed improved affinity and antagonism compared to $R^2 = H$, but the effect is not as great as with $R^2 = OMe$.

Combining the optimized substituents in Tables 1 and 2 produces the initial entries in Table 3. Starting with **19** and maintaining the OMe group on the central phenyl ring, an increase in affinity is seen with **25** where $R^1 = (3-Cl)Ph$ and $R^3 = 2$ -pyrimidine. Continued improvement of both the biological and the physicochemical profile is seen when $R^1 = R^3 = 2$ -pyridine (**26**). Not only does **26** show potent affinity (K_i : 21 nM) and antagonism (IC_{50} : 8 nM), but it has good aqueous solubility (50 $\mu g/mL$), a good CYP profile (37, 1, 16) and improved RLM stability ($t_{1/2}$: 23 min). This is consistent with the improved LipE (4.5) seen with this compound. The effect of $R^2 = OMe$ versus $R^2 = H$ is seen with **26** in comparison to compound **15** which is less potent than **26** and

possesses a shorter RLM $t_{1/2}$. Close analogs of **26** with similar LipEs also show good affinity/antagonism and good physicochemical profiles. Besides 2-pyridine (**26**, **27**), R^1 can be 6-Me-2-pyridine (**28**) or 2-thiazole (**29**). In addition to 2-pyridine (**26**, **28–29**), R^3 can be 2-pyrimidine (**27**) and 5-Me-2-pyridine (**30**).

Based on its excellent mGluR5 affinity, antagonism and its excellent properties profile, compound **26** was selected for PK/brain exposure evaluation (Table 4). PK studies were performed in Swiss Webster mice, Sprague–Dawley rats and beagles at 2 mpk, iv and 10 mpk, po. In general, rat and dog showed similar 2 mpk, iv PK profiles: moderate clearance (rat: 12 mL/mg/min; dog: 3 mL/mg/min), moderate volumes of distribution (rat: 0.9 L/kg; dog: 0.5 L/kg) and short half-lives (rat: 1 h, dog: 2.1 h). Mouse on the other hand showed much higher clearance (121 mL/mg/min), a larger volume of distribution (3.2 kg/K) and a shorter half-life (0.2 h). This difference is consistent with the microsomal stability data for these species which shows that **26** has a shorter $t_{1/2}$ in mouse microsomes (5 min) compared to rat or human microsomes (23

Table 2
 R^2 4-phenyl and R^3 -piperazine mGluR5 negative allosteric modulator derivatives **1**, **16–24**



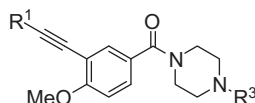
1, **16–24**

Compds	R^2	R^3	mGluR5 K_i^a (nM)	mGluR5 IC_{50}^a (nM)	Aq solubility ($\mu g/mL$)	CYP inhibition, 3A4, 2D6, 2C9 (% inhib. @ 3 μM)	RLM stability, $t_{1/2}$ (min)	LipE ^b
1	H	2-Pyridine	139	926	0.5	48, 5, 50	3	2.4
16	H	2-Pyrazine	401	1378	3	22, 9, 35	4	2.7
17	H	2-Pyrimidine	451	nd	2	0, 12, 75	3	2.7
18	H	5-Me-2-pyridine	65	181	1	45, 10, 67	13	2.2
19	OMe	2-Pyridine	19	40	1	61, 5, 55	13	3.0
20	OMe	2-Pyrazine	27	nd	2	62, 7, 34	5	3.7
21	OMe	2-Pyrimidine	62	46	2	14, 10, 53	21	3.3
22	OMe	5-Me-2-pyridine	3	40	1	54, 8, 72	16	3.3
23	Me	2-Pyridine	59	nd	1	58, 11, 69	13	2.3
24	Me	2-Pyrazine	145	192	3	45, 18, 50	9	2.6

^a Values are means of two experiments, standard deviations are $\pm 10\%$.

^b LipE is calculated using mGluR5 IC_{50} values.

Table 3
 R^1 terminal alkyne and R^3 -piperazine mGluR5 negative allosteric modulator derivatives **19**, **25–30**



19, **25–30**

Compds	R^1	R^3	mGluR5 K_i^a (nM)	mGluR5 IC_{50}^a (nM)	Aq solubility ($\mu g/mL$)	CYP inhibition, 3A4, 2D6, 2C9 (% inhib. @ 3 μM)	RLM stability, $t_{1/2}$ (min)	LipE ^b
19	Ph	2-Pyridine	19	40	1	61, 5, 55	13	3.0
25	(3-Cl)Ph	2-Pyrimidine	5	66	1	73, 5, 43	7	4.1
26	2-Pyridine	2-Pyridine	21	8	50	37, 1, 16	23	4.5
27	2-Pyridine	2-Pyrimidine	30	nd	>100	44, 34, 14	18	5.1
28	6-Me-2-pyridine	2-Pyridine	35	14	18	27, 18, 28	11	3.8
29	2-Thiazole	2-Pyridine	24	6	29	52, 24, 33	15	4.6
30	2-Pyridine	5-Me-2-pyridine	19	31	19	24, 0, 29	> 30	4.1

^a Values are means of two experiments, standard deviations are $\pm 10\%$.

^b LipE is calculated using mGluR5 IC_{50} values.

Table 4
PK/Exposure profile of compound **26**

		SW Mouse	SD Rat	Dog
2 mpk iv	CL (mL/min/kg)	121	12	3
	V_{ss} (L/kg)	3.2	0.9	0.5
	$t_{1/2}$ (h)	0.2	1	2.1
10 mpk po	C_{max} (μ M)	3.5	11.9	16.4
	AUC _{last} (h*ng/mL)	519	13,375	47,075
	%F	20	85	80
	B/P	0.31	0.15	—
	C_{max} brain (μ M)	1.09	1.79	—
	Fu brain	0.13*	0.13	—
	Cfu brain (μ M)	0.14*	0.23	—

* Assumes Fu brain is rat ~ Fu brain in mouse.

and 21 min). The 10 mpk, po PK profiles also show the same species comparisons as seen with the iv PK. The mouse C_{max} and AUC_{last} values (3.5 μ M, 519 h*ng/mL) are lower than the corresponding values for rat and dog (rat: 11.9 μ M, 13,375 h*ng/mL; dog 16.4 μ M, 47,085 h*ng/mL). The oral bioavailability in these species ranged from moderate (20% in mouse) to excellent (85% in rat; 80% in dog).

Brain exposure studies were performed with **26** in mouse and rat. In both species at 10 mpk, **26** showed similar brain penetration ratios (mouse: 0.31; rat 0.15) which based on the plasma C_{max} translates to C_{max} brain levels of 1.09 μ M for mouse and 1.79 μ M for rat. Protein binding studies for **26** in rat brain homogenate indicates that the Fu for **26** in brain is 0.13. Assuming the Fu for mouse is similar, the mouse brain Cfu is calculated to be 0.14 μ M, a

concentration which is well above its measure mGluR5 K_i and IC₅₀ values (K_i : 21 nM; IC₅₀: 8 nM).

Given its good PK and brain exposure, **26** was assessed in the mouse 4-Plate (Fig. 1) and mouse SIH (Fig. 2) rodent models.¹³ In the 4-Plate assay, ip administration resulted in a statistically significant increase in punished crossings at 1 and 3 mpk. The number of punished crossings at 0.3 mpk is similar to that seen in the vehicle group (Fig. 1A). With po dosing (Fig. 1B), statistically significant increases in punished crossings were observed at 30 mpk with a strong trend towards increased punished crossing observed at 10 mpk ($p = 0.06$). As mentioned above, the maximal brain exposure for **26** at 10 mpk, po is roughly 17-fold above the mGluR5 IC₅₀ for this compound (140 nM exposure: IC₅₀: 8 nM). Similar efficacy was observed in the SIH model. Following ip administration (Fig. 2A), **26** produced a statistically significant attenuation of the hyperthermic response at 3 and 10 mpk. At 1 mpk ip, a trend towards a reduction in the hyperthermic response was also observed. Following po administration (Fig. 2B), there was a statistically significant attenuation of the hyperthermic response observed at 17.8 mpk with a strong trend at 10 mpk ($p = 0.07$). Thus **26** demonstrated robust activity in two models predictive of anxiolytic-like efficacy in vivo. Exposure data is consistent with these effects being governed by high mGluR5 receptor occupancy.

We have shown that careful optimization of HTS hit **1** while paying attention to LipE led to a highly potent and efficacious series of mGluR5 NAMs (from LipE for **1**: 2.4, to LipE for **15**, **25–27** and **29–30**: >4.1). One example **26** showed good PK profiles in rat and dog and good brain exposure in rat. 4-Plate and SIH models of anxiety showed statistically significant efficacious activity with MEDs

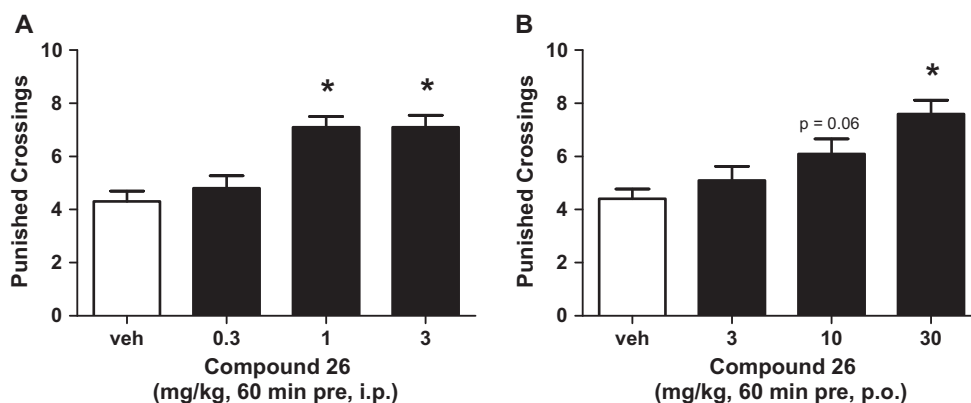


Figure 1. Mouse 4-Plate Behavioral assay using Compound **26** showing minimum efficacious doses (MEDs) of (A) 1 mpk, ip, 60 min compound pretreatment and (B) 30 mpk, po, 60 min compound pretreatment.

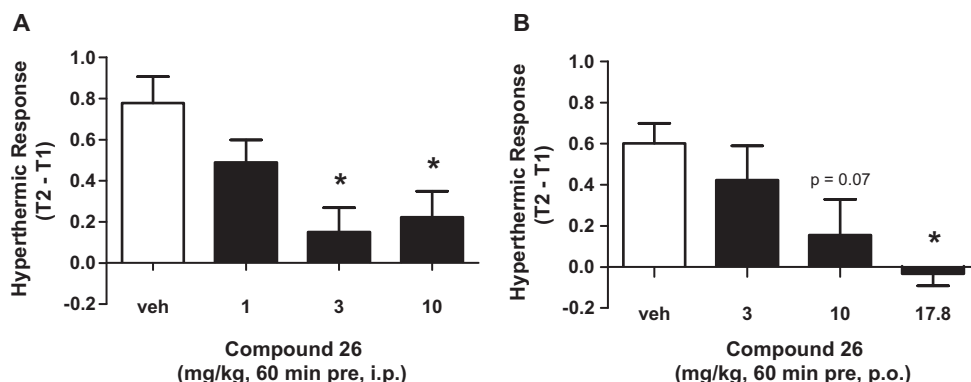


Figure 2. Mouse Stress Induced Hyperthermia assay Using Compound **26** showing minimum efficacious doses (MEDs) of (A) 3 mpk, ip and (B) 17.8 mpk, po.

of 10 mpk, po in both assays. The continued optimization of this series of mGluR5 NAMs will be presented in due course.

Acknowledgements

We thank the Wyeth Compound Properties group for the generation of the HT-physicochemical properties reported in this manuscript. We also would like to thank Dr. Steven V. O'Neil of Pfizer Global Research and Development for his input into this manuscript.

References and notes

1. Malherbe, P.; Kratochwil, N.; Muhlemann, A.; Zenner, M. T.; Fischer, C.; Stahl, M.; Gerber, P. R.; Jaeschke, G.; Porter, R. H. *J. Neurochem.* **2006**, *98*, 601.
2. Schoepp, D. D.; Jane, D. E.; Monn, J. A. *Neuropharmacology* **1999**, *38*, 1431.
3. Romano, C.; Sesma, M. A.; McDonald, C. T.; O'Malley, K.; Van den Pol, A. N.; Olney, J. W. *J. Comp. Neurol.* **1995**, *355*, 455.
4. Valenti, O.; Conn, P. J.; Marino, M. J. *J. Cell. Physiol.* **2002**, *191*, 125.
5. Lindsley, C. W.; Emmitte, K. A. *Curr. Opin. Drug Discov. Devel.* **2009**, *12*, 446.
6. All newly prepared compounds were characterized by ¹H NMR and reversed phases-HPLC/MS spectroscopy.
7. Christiansen, E.; Urban, C.; Merten, N.; Liebscher, K.; Karlsen, K. K.; Hamacher, A.; Spinrath, A.; Bond, A. D.; Drewke, C.; Ullrich, S.; Kassack, M. U.; Kostenis, E.; Ulven, T. *J. Med. Chem.* **2008**, *51*, 7061.
8. Rich, D. H.; Singh, J. *Peptides (NY)* **1979**, *1*, 241.
9. Erdelyi, M.; Gogoll, A. *J. Org. Chem.* **2001**, *66*, 4165.
10. Tobe, Y.; Utsumi, N.; Kawabata, K.; Nagano, A.; Adachi, K.; Araki, S.; Sonoda, M.; Hirose, K.; Naemura, K. *J. Am. Chem. Soc.* **2002**, *124*, 5350.
11. Kerns, E. H.; Di, L. *Drug-Like Properties: Concepts, Structure Design and Methods: from ADME to Toxicity Optimization*; New York: Academic Press, 2008.
12. Ryckmans, T.; Edwards, M. P.; Horne, V. A.; Correia, A. M.; Owen, D. R.; Thompson, L. R.; Tran, I.; Tutt, M. F.; Young, T. *Bioorg. Med. Chem. Lett.* **2009**, *19*, 4406.
13. Hughes, Z. A.; Liu, F.; Platt, B. J.; Dwyer, J. M.; Pulicicchio, C. M.; Zhang, G.; Schechter, L. E.; Rosenzweig-Lipson, S.; Day, M. *Neuropharmacology* **2008**, *54*, 1136.